Ocean Engineering 305 (2024) 118026

Contents lists available at ScienceDirect

Ocean Engineering

journal homepage: www.elsevier.com/locate/oceaneng

AIS-based kinematic anomaly classification for maritime surveillance

Jinliang Liu [a], Jianghui Li [a,b,*], Chunshan Liu [c]

[a] College of Ocean and Earth Sciences, Xiamen University, Xiamen, Fujian, China
[b] State Key Laboratory of Marine Environmental Science, Xiamen University, Xiamen Fujian, China
[c] School of Communication Engineering, Hangzhou Dianzi University, Hangzhou, Zhejiang, China

ARTICLE INFO

Keywords:
AIS data
Kinematic anomaly detection
Maritime surveillance

ABSTRACT

Anomaly detection is crucial for maritime surveillance and law enforcement. Early identification of abnormal behavior ensures maritime order and fosters a safer environment for maritime traffic. However, anomaly identification and classification methods often suffer from vagueness because of the complexity of anomalies, limiting their effectiveness. We propose a systematic and data-driven framework for kinematic anomaly classification and detection. Through extensive inspection and experiments, a comprehensive characterization of diverse anomalies is provided to classify vessel kinematic anomalies into three categories, including Speed and Course Anomaly (SCA), Turning Anomaly (TA) and Loitering Anomaly (LA), along with detection methods that are tailored to each anomaly type to facilitate the production of high-quality anomaly labels. Subsequently, supervised training is exploited for anomaly classification. The effectiveness of the proposed method is validated using the open Automatic Identification System (AIS) dataset provided by the Danish Maritime Authority (DMA). With proper feature design, the proposed method can achieve a classification accuracy of approximately 99% using simple neural networks.

1. Introduction

With more than 80% of all global trade handled by marine vessels nowadays (UNCTAD, 2022), maritime traffic data has been increasingly crucial for maritime surveillance and safety. As the increase in maritime trade turns the oceans into crowded thoroughfares, traffic accidents have become more common in these busy marine routes. Allianz Safety & Shipping Review 2023 (AGCS, 2023) reveals that the total number of shipping casualties or incidents reached 3032 in 2022, compared to 2698 accidents reported in 2018, indicating a 12% increase. Given this escalation in ship accidents, maritime traffic safety shall be prioritized, and effective vessel surveillance must be emphasized. Early identification of suspicious vessel behavior allows maritime regulatory authorities to take prompt actions to minimize damage and reduce casualties (Ribeiro et al., 2023). Hence, anomaly detection stands out as a critical aspect of maritime situational analysis (MSA), focusing on identifying unusual or unexpected vessel behavior, such as trajectories deviating from the typical or anticipated patterns (Ferreira et al., 2022; Roy, 2008).

Under the guidelines set by the International Maritime Organization (IMO) in the Safety of Life at Sea (SOLAS) convention of 1980 (IMO, 1980), it is compulsory for vessels of specific types and sizes to be equipped with an Automatic Identification System (AIS). This mandate is intended to improve safety in maritime traffic. AIS devices facilitate vessel tracking through static and dynamic data. Static data includes vital information about the vessel, such as Maritime Mobile Service Identity (MMSI), ship name, ship type, length, etc. Dynamic data contains position information such as longitude (LON) and latitude (LAT), as well as maneuvering data such as speed over ground (SOG), course over ground (COG), heading, etc. Dynamic messages are reported every 2 to 12 s, while static messages are reported every 6 min.

In recent years, the maritime traffic industry has been evolving towards higher computational capabilities and artificial intelligence (Chen et al., 2023, 2024). The abundance of vessel movement data within the AIS system has significantly expanded its applications, which includes trajectory clustering (Li et al., 2018; Park et al., 2021; Wang et al., 2021; Xu et al., 2023), trajectory prediction (Capobianco et al., 2021; Xu et al., 2022), maritime traffic monitoring (Arguedas et al., 2018), vessel behavior analysis (Bye and Aalberg, 2018), environmental evaluation (Winther et al., 2014), path planning (Zhou et al., 2020) and especially anomaly detection (Nguyen et al., 2022; Zhao and Shi, 2019; Pallotta et al., 2013a,b). The increasing volume of AIS data has made these tasks both feasible and challenging. Efficient utilization depends on the implementation of appropriate filtering and preprocessing techniques.

Anomalies are generally characterized as irregular and unexpected events and manifest as rare and stochastic occurrences. In the maritime

* Corresponding author.
E-mail addresses: liujinliang@stu.xmu.edu.cn (J. Liu), jli@xmu.edu.cn (J. Li), chunshan.liu@hdu.edu.cn (C. Liu).

https://doi.org/10.1016/j.oceaneng.2024.118026
Received 30 January 2024; Received in revised form 18 April 2024; Accepted 24 April 2024
Available online 27 April 2024
0029-8018/© 2024 Elsevier Ltd. All rights reserved.

geographical context, shipping activities are often influenced by the marine environment, and an adverse geographical environment is challenging for ship operators (Chen et al., 2022). So anomalies are closely linked to the surrounding environment. Furthermore, one anomaly often accompanies others, which adds complexity to exhaustively identify and characterize each category of anomalous behavior. The spatio-temporal dependencies among data within various regions of the road network exhibit intricate dynamics (Xiao et al., 2023). Similar to road networks, maritime traffic network data is inherently dynamic, but its complexity surpasses that of road networks. This complexity arises from the absence of road constraints, making it more challenging to reveal vessel motion patterns and detect anomalies.

In anomaly classification, anomalies are concluded into unexpected changes in speed or location, position anomaly, etc (Sidibé and Shu, 2017). More systematically, some researchers classify vessel anomalous behavior into five categories: (i) positional anomalies, i.e., vessels deviating from the designed channels, (ii) contextual anomalies, i.e., anomalies related to seasons, (iii) kinematic anomalies, i.e., anomalies concerned with speed and course, (iv) complex anomalies, i.e., vessels with loitering or spoofing behavior, and (v) data-related anomalies, i.e., vessels with incomplete trajectory data (Riveiro et al., 2018).

Positional anomalies, kinematic anomalies, and data-related anomalies can be detected through AIS data exclusively. Among these categories, kinematic anomaly is one of the most complicated categories and contains a large amount of distinct anomalous behavior on the speed and course of vessels. Examples include unusually high/low speed, abnormal course changes, and abrupt stops and turns. Given loitering behavior is primarily induced by abnormal speed and course of the vessel, we categorize it as part of kinematic anomalies. To the best of our knowledge, there has been no systematic classification of kinematic anomalies. Previous studies have predominantly relied on simple descriptions (Davenport, 2008; Guo et al., 2021), whereas our classification approach is anchored in identifying anomalous features.

Identifying kinematic anomalies is essential for ensuring maritime security and preventing illegal activities to mitigate potential dangers; however, the detection of these anomalies of vessels is challenging. One core reason is that the further classification of kinematic anomalies is intricate with massive subtypes while it lacks a systematic characterization of these anomalous patterns. As a result, there persists a scarcity of publicly available labeled data for kinematic anomaly detection since it is difficult to establish the ground truth without a systematic characterization of the anomalous behavior. This limitation has led to the prevalent use of unsupervised methods in most machine learning solutions to this task (Chandola et al., 2009). Without the ground truth, these methods cannot achieve a thorough comprehension of the intrinsic characteristics of distinct anomalies. Despite their capability to detect abnormal patterns, the approaches lack interpretability for the results and eventually lead to a high misclassification rate.

In this paper, we propose a new and systematic vessel anomaly detection framework for kinematic anomalies. Diverging from previous studies, our research begins with a formal and comprehensive classification and characterization of these anomalies. We classify them into three primary types and explore their interrelationships subsequently. To establish a labeled dataset of anomalies, we investigate different anomalies according to the detection rules tailored to each anomaly type. Ultimately, the supervised learning approach is applied to learn the relationship between samples and labels to accomplish the classification task.

The contribution of this work is as follows:

(1) We propose a detailed classification method of kinematic anomalies in vessels, categorizing them into three types;
(2) We introduce a novel framework for identifying kinematic anomalies, aimed at translating our knowledge of various anomalies into distinct detection rules and detecting the anomalies within AIS data;
(3) We present a comprehensive and high-quality dataset of kinematic anomalies in vessel behavior, which can serve as ground truth for anomaly detection.

The paper is organized as follows. In Section 2, we present an overview of the related work. Section 3 demonstrates the proposed framework. Section 4 presents the experimental results on historical AIS data. In Section 5, conclusions and discussions are summarized.

2. Related work

Recently, an increasing number of studies have made notable advancements in detecting anomalous behavior in vessels (Pallotta and Jousselme, 2015; Rong et al., 2020). Despite these efforts, the overall scope of research in this field remains constrained. A principal factor contributing to this limitation is the absence of a comprehensive dataset for anomalies, a deficiency stemming from the challenges associated with precise anomaly classification and the provision of detailed descriptions.

Traditional anomaly detection methods generally involve normalcy modeling, followed by deviation estimation between test samples and the constructed model. Subsequently, the detection methods identify anomalies by comparing the deviation to a predefined threshold, and they regard any deviation from it as an anomaly. Anomaly detection approaches can be classified into three types: statistical methods, machine learning approaches, and neural networks.

Statistical methods, such as Gaussian Mixture Model (GMM) and Kernel Density Estimator (KDE) (Laxhammar et al., 2009; Anneken et al., 2015) are commonly employed for maritime traffic pattern modeling; however, their performance often falls short, marked by high rates of missed detections and false alarms. An alternative approach proposed by Mascaro et al. (2014) involves Bayesian Networks to enhance model performance. A model based on the Hidden Markov Model (HMM) is designed to create individual HMM models for each behavior of vessels to classify their trajectories (Toloue and Jahan, 2018). While statistical models do not require additional prior knowledge of vessel motion patterns, these techniques may be constrained when applied to larger regions, particularly in capturing heterogeneous motion patterns (Pallotta et al., 2013a). To address this, grid-based solutions have been proposed (Laxhammar, 2008; Rhodes et al., 2007), enabling a detailed analysis of vessel motion characteristics without losing local features.

Clustering is essential in machine learning for maritime anomaly detection, and Density-Based Spatial Clustering of Applications with Noise (DBSCAN), especially plays a vital role. The core idea of detecting anomalies with clustering is to identify crucial traffic points and routes as reference patterns and measure the similarity between test trajectories and these patterns. A framework named TREAD, which utilizes DBSCAN to extract distinct patterns, is proposed (Pallotta et al., 2013a). The identification of potential abnormal behavior relies on the comparison of consistency. The effectiveness of anomaly identification in clustering algorithms depends on similarity metrics. To deal with the complexities of maritime traffic situations, a hybrid similarity metric that combines three division distances is designed (Liu et al., 2015). However, it is important to note that DBSCAN is sensitive to hyperparameter settings (such as Eps, the radius of the clusters, and MinPts, the minimum number of points in a cluster). Moreover, DBSCAN demands intricate computations or domain expertise, with a time complexity of $O(n^2)$ (Sidibé and Shu, 2017). Besides clustering algorithms, supervised algorithms like support vector machines (Handayani et al., 2013) are also frequently employed.

A system named GeoTrackNet is created for unsupervised anomaly detection (Nguyen et al., 2022). It represents AIS information by considering four key trajectory features: latitude, longitude, speed, and course, which are encoded and uniquely resembling one-hot encoding. The Variational Recurrent Neural Network (VRNN) is utilized to establish a probabilistic normalcy model for capturing trajectory variations.

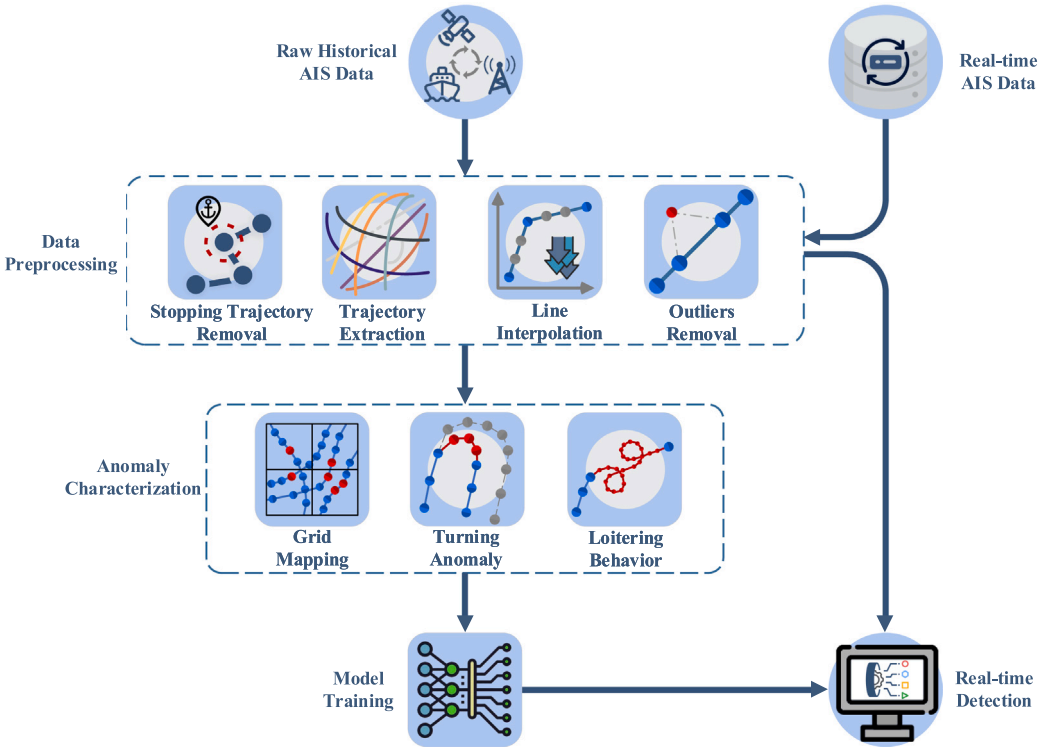

Fig. 1. Workflow map of kinematic anomaly detection model training and real-time data analysis: (1) Raw AIS data undergoes four processing steps to filter and reduce data volume; (2) Anomaly characterization is performed on the extracted trajectories for anomaly detection; (3) A supervised model for anomaly classification is trained with labeled trajectory data; (4) Real-time detection is implemented after data preprocessing using the trained model.

Ultimately, it exploits a geospatial detector for anomaly detection and yields significant results. While the model proves effective in identifying certain anomalies, it cannot specify the exact anomaly type and opts to generalize them as anomalies, where human effort is indispensable for final decision-making.

Here, our objective is to address challenges related to the detection and classification of kinematic anomalies in maritime vessels and the accuracy of anomaly detection by establishing a systematic model for detecting distinct kinematic anomalies in vessels, acquiring a robust anomaly dataset, and improving the interpretability of anomalous results.

3. Methodology

In this section, we describe the methodology of the proposed anomaly detection system. Fig. 1 displays the overall workflow of the framework. The system consists of two paths: model training with historical AIS data and real-time data analysis. The former comprises three integrated modules: data preprocessing, anomaly identification, and model training. Once the model completes its training, it is locally stored and immediately deployed for real-time data analysis upon processing incoming data streams. This framework leverages the advantages of the pre-trained models, ensuring a streamlined and effective detection mechanism.

3.1. Data preprocessing

The volume of raw AIS data is enormous with numerous fields. Various data errors, such as duplicate records, missing values, outliers, and invalid data still exist. Therefore, data cleaning and filtering are essential for subsequent analysis.

Step-1: **Pre-filtering and stopping trajectory removal**. First of all, entries with logical errors or missing values are excluded. Then we select the records within the area of interest (AOI). Stopping trajectories, where vessels are berthed or anchored within approximately five kilometers of the dock, are also excluded.

Step-2: **Trajectory extraction**. AIS data entries with the same MMSI are initially grouped together and then sorted chronologically to form a candidate trajectory. To address potential large gaps that naturally divide the candidate trajectories into disjointed trajectory segments, a segmenting approach based on both distance and time gaps is employed. Specifically, the extracted trajectory must meet the following criteria:

(1) Contiguous points have a maximum gap $\leq$2 h;
(2) Distance between two adjacent points $\leq$5 km;
(3) Duration of each trajectory lasts $\geq$6 h;
(4) Points of each trajectory $\geq$20.

Trajectories that do not meet conditions (1) or (2) must be segmented at the existing intervals, while those failing the latter two criteria are discarded.

Step-3: **Line interpolation**. After *Step-2*, the extracted trajectories may have uneven intervals spanning from a few seconds to several minutes. Since vessels' navigational states do not change drastically in the short term, down-sampling is remarkably beneficial to reduce the data volume without introducing excessive alterations to trajectory shapes. Thus, we employ linear interpolation to re-sample Timestamp, LON, LAT, COG, and SOG. The resampling interval is set to 150 s to balance data volume and the precision of trajectories.

Step-4: **Outlier removal**. We exclude the outliers based on a maximum vessel speed of 30 knots. Points with an average speed exceeding this threshold, calculated as the ratio of geographical distance to the interval between consecutive points, are considered outliers and removed from these trajectories.

3.2. Kinematic anomaly classification

Upon extensive inspection of a large number of kinematic anomalous samples, a shared pattern emerged. That is, most anomalies exhibit

distinct changes in both speed and course, with variations attributed to the primary factor contributing to their occurrence. We categorize these anomalies into three main types: Speed and Course Anomaly (SCA), Turning Anomaly (TA), and Loitering Anomaly (LA). Motivated by the utilization of four-hot vector for anomaly detection (Nguyen et al., 2022), we focus on time-series characteristics of LON, LAT, SOG, and COG of these trajectories.

SCA is defined by abnormal changes in both speed and course, and it is the most prevalent anomaly. TA occurs when a vessel, not operating at low speed, executes a turn with a radius smaller than the specified value, typically the minimum safe turning radius. As for LA, numerous studies have investigated the loitering behavior of other traffic entities, such as pedestrians and vehicles. However, it lacks a precise definition of vessel loitering behavior in the maritime domain, making its identification process rather ambiguous. We describe them as vessel activities without an obvious purpose within a restricted range, often featuring repeated motion patterns.

It is noteworthy that there is overlap among these three anomaly types. For instance, when a vessel maneuvers in circular patterns, it manifests TA and simultaneously shares similarities with LA. Besides, sharp turns often result in both SCA and TA. Consequently, a single trajectory may exhibit multiple types of anomalies, presenting considerable challenges in building a model with robust classification performance.

To enhance the efficiency of trajectory anomaly classification, it is crucial to establish clear boundaries between distinct anomaly types. Loitering events refer to instances in which a vessel maintains speeds below 2 knots during solo operations (Miller et al., 2018). Thus, we adopt the same definition as the speed ceiling threshold of LA. TA, on the other hand, occurs when the vessel's speed is above 2 knots.

Additionally, a potential hierarchy of weight relationships exists. While these three categories share the abnormal characteristics in speed and course, the immediate causes of TA and LA are the abnormal turning and loitering behavior respectively, which introduce additional features to the anomalies. Therefore, when either TA or LA coincides with SCA, the trajectory is labeled as a TA or LA instead of a SCA, to reflect more accurately its root cause and significance.

3.3. Kinematic anomaly characterization and identification

In this subsection, we formally present the characterization of the three types of kinematic anomalies defined above and the corresponding procedures for anomaly identification. The results of anomaly identification serve as robust ground truth for training a neural network-based anomaly detection system in a supervised manner. Before delving into the details of the anomaly characterization, we introduce the following notations.

Vessel's track, denoted as trajectory T, consists of a sequence of timestamped points, e.g. $T = \{P_1, P_2, \ldots, P_n\}$, where $P_i = \{timestamp_i, lon_i, lat_i, cog_i, sog_i, \ldots\}$, $for\, i = 1{:}\ n$. Here P_i represents the i-th point from trajectory T made up of N points, and $timestamp_i, lon_i, lat_i, cog_i, sog_i$ represent timestamp, longitude, latitude, course, and speed respectively. Each point P is composed of these key attribute values.

3.3.1. SCA detection

A procedure based on geographic grids is applied to identify SCA. Grid-based methods can divide the research area into grids and cluster trajectory points using the density of each grid to capture movement behavior (Lei et al., 2011). Hence, we utilize grid mapping methods for vessel motion pattern extraction.

First, focusing on variations in SOG and COG, we compute the differences between consecutive points in each trajectory, referred to as the rate of change in SOG and COG. These can be calculated as follows:

$$a_i = \begin{cases} \frac{SOG_i - SOG_{i-1}}{\Delta t}, \text{if } i \geq 2 \\ 0 \qquad\qquad\quad, \text{if } i = 1 \end{cases} \tag{1}$$

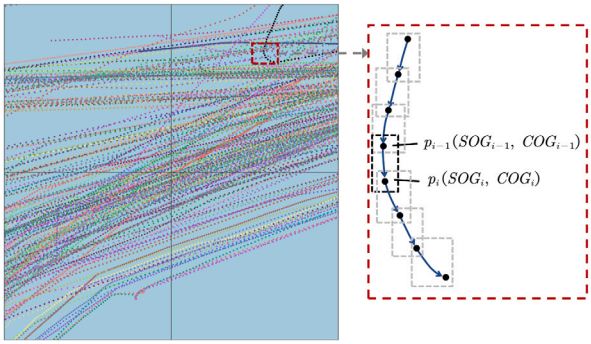

Fig. 2. Illustration of the grid mapping method for SCA detection: Trajectory points are separated into defined grid cells, and the change rates of SOG and COG between consecutive points p_{i-1} and p_i along the trajectory are calculated per grid.

$$\omega_i = \begin{cases} \frac{COG_i - COG_{i-1}}{\Delta t}, \text{if } i \geq 2 \\ 0 \qquad\qquad\quad, \text{if } i = 1 \end{cases} \tag{2}$$

where a_i and ω_i are the rate of change in SOG and COG for point P_i in the calculated trajectory. The values SOG_{i-1} and COG_{i-1} are extracted from P_{i-1}, while SOG_i and COG_i are from P_i. Δt is the interval between contiguous points. And a_1 and ω_1 are set to 0, indicating the initial state. An appropriate grid size is chosen afterward, as shown in Fig. 2, to partition the observed area into smaller grid cells with equal length and width. The points from trajectories are then projected into these grids.

A widely adopted method for outlier detection involves identifying data points as outliers if their deviation from the mean μ exceeds 3σ, where σ denotes the standard deviation. The range, defined by $\mu \pm 3\sigma$, covers roughly 99.7% of the data instances (Chandola et al., 2009). When a sufficient number of trajectory points fall into the grid cells, the data distribution can be approximated as following a Gaussian distribution $\xi \sim \mathcal{N}(\mu, \sigma^2)$. The values of ξ are predominantly concentrated within the interval between $(\mu - 3\sigma, \mu + 3\sigma)$. Hence, the normal range is established using the mean and variance of a and ω:

$$a_i \in (\overline{a} - 3\sigma_a, \overline{a} + 3\sigma_a), \tag{3}$$

$$\omega_i \in (\overline{\omega} - 3\sigma_\omega, \overline{\omega} + 3\sigma_\omega). \tag{4}$$

The method examines each trajectory point to classify it as normal or anomalous based on the specified bounds. If two consecutive points share the same grid, their associated statistical values are used directly; otherwise, when spanning different grids, the normal data range is calculated by averaging the statistical values of the respective grids.

Note that the normal range may need adjustments under certain conditions. When there is a low number of trajectory points projected onto a grid cell, or when points are highly concentrated within a cell, the validity of interval boundaries may be compromised. To address this, we set a minimum threshold for standard deviation as a safety measure to prevent mistaken classification of normal trajectory points.

As depicted in Fig. 3, a representative anomaly occurs during the latter part of the vessel's voyage when it abruptly initiates a braking and steering maneuver, with drastic changes in SOG and COG. This unexpected behavior could be attributed to a potential encounter with an obstruction along its course. Such sudden alterations in speed and heading are prone to triggering accidents, especially in busy waterways, posing a significant risk. The representative trajectory segments with SCA, illustrated in Fig. 4, exhibit distinctive motion patterns, resulting in peculiar trajectory shapes.

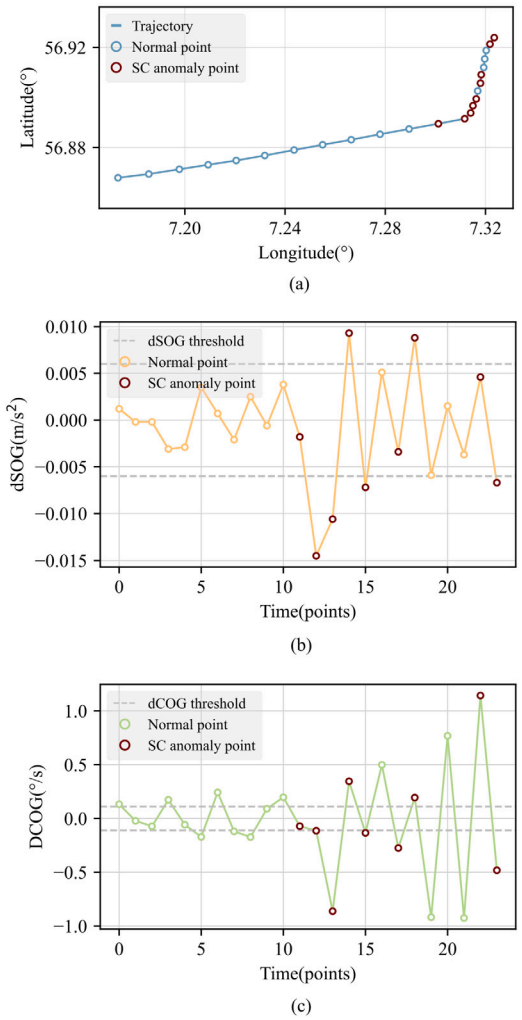

Fig. 3. Example of an SCA: (a) The trajectory segment exhibiting SC anomalous behavior, with red spots representing SCA points; (b) and (c), graphs of SOG and COG change rate. Gray dashed lines represent the change rate threshold. The segments between adjacent red points indicate trajectory portions with anomalies, and red dots denote anomalous points.

3.3.2. TA detection

To capture TA, a point-based curvature calculation method is employed. The curvature is measured by calculating the reciprocal of the radius of the circumscribed circle formed by three consecutive points, denoted as P_{i-1}, P_i, P_{i+1}, where P_i is the point under consideration and P_{i-1}, P_{i+1} are its two neighboring points. The process is illustrated in Eq. (5):

$$\kappa = \frac{2\sin\alpha}{L}. \tag{5}$$

where, α represents the angle between $\overrightarrow{P_{i-1}P_i}$, $\overrightarrow{P_iP_{i+1}}$ or $\overrightarrow{P_iP_{i+1}}$, $\overrightarrow{P_{i-1}P_{i+1}}$, and L being length of the side opposite to α. Distances are calculated using the Haversine formula. This curvature calculation is crucial for evaluating a vessel's turning behavior.

The detection threshold for TA is specifically established for each vessel. The turning radius, which is the inverse of curvature and represents the radius of the narrowest circle within which a vessel can complete a full turn safely, is closely associated with the length of the vessel. If TA arises, indicating a sharp turn, the vessel may be put at risk of capsizing, simultaneously affecting the regular navigation of others. To enhance the precision in quantifying the turning radius or curvature, insights from British Standards Institution (BSI, 2013)

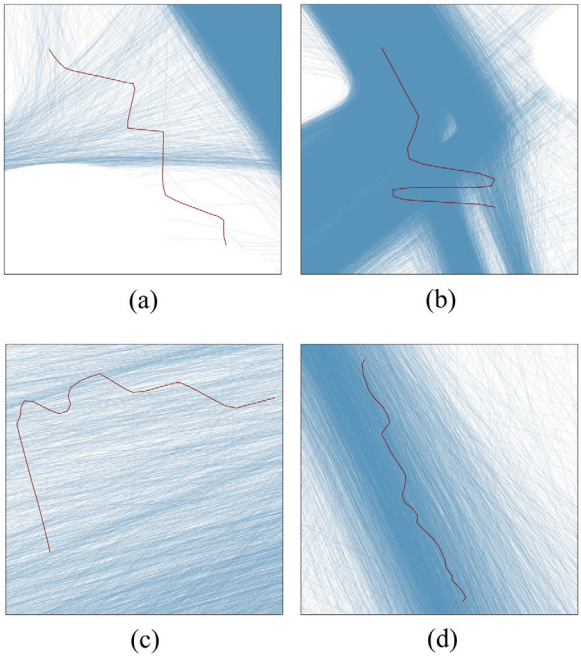

Fig. 4. Representative trajectory segments with SCA caused by an unusual change rate of both speed and course; Red lines: trajectory segments with SCA; Blue lines: trajectories with normal motion patterns.

suggest a connection between the maximum turning curvature and the vessel length can be described as:

$$\kappa \leq \frac{1}{k * length}. \tag{6}$$

where κ represents the curvature of each trajectory point, and k is set to be 2. If the local curvature of a point exceeds the threshold, the point and its two neighboring points are considered anomalous points.

Fig. 5 presents four representative trajectories exhibiting anomalous motion patterns while turning, completely different from the normal navigation states of other vessels, which pose extreme risks to maritime traffic.

3.3.3. LA detection

As we can gather, LA represents the most complicated and challenging category within kinematic anomalies for its elusive motion patterns. The characteristics of loitering trajectories are straightforward to identify (Wijaya and Nakamura, 2023), which are as follows:

- Slow velocity: When a vessel is moving at a slow speed, it may be loitering;
- Frequent course alterations: When a vessel changes course frequently, it may suggest loitering;
- Limited traveling distance over a period: When a vessel covers a minimal distance within a specific time frame, it may indicate loitering;

However, it is difficult to effectively detect LA using predefined rules. Therefore, we opt to acquire reliable loitering trajectories through manual annotation. We initiate a preliminary screening on the COG variance of the entire trajectory, followed by a detailed assessment and classification according to the specified characteristics of loitering behavior.

Loitering trajectory segments exhibit various spatial shapes. Representative loitering shapes can be categorized into four types: disordered retracing shape with reciprocating patterns, lasso shape, systematic back-and-forth pattern, and irregular coil shape (Zhang et al., 2022).

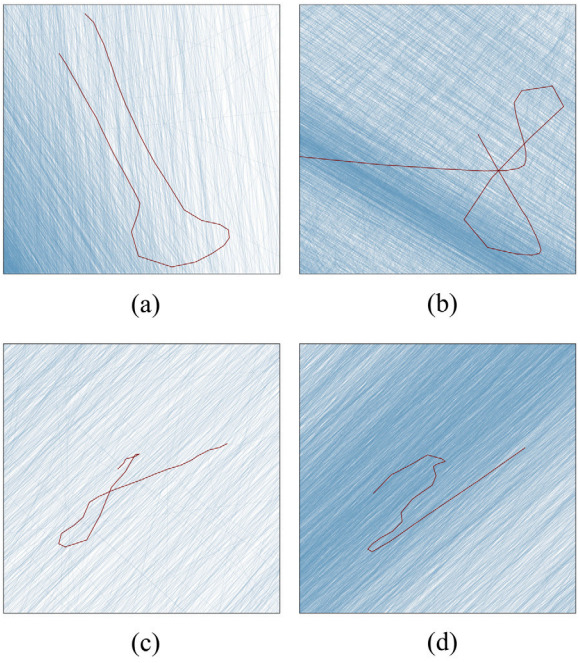

Fig. 5. Representative trajectory segments with TA caused by abrupt turning behavior; Red lines: trajectory segments with TA; Blue lines: trajectories with normal motion patterns.

Table 1
Category-label mapping table.

Category	Label
Normal	0
SCA	1
TA	2
LA	3

Additionally, we identify another shape of loitering trajectory and name it the zigzagging shape. As presented in Fig. 6, the LA examples of three shape types are detected and labeled. These loitering behaviors may result from adverse weather conditions, mechanical failures, pirate attacks, smuggling activities, etc. Therefore, timely detection of loitering behavior is crucial for maritime surveillance.

3.4. Supervised learning-based anomaly detection

The method discussed in Section 3.3 provides a convenient way to label kinematic vessel trajectory anomalies and as a result the high-quality anomaly dataset which can be utilized to train an anomaly classifier in a supervised manner. In this section, we present a brief overview of the process. Specifically, both normal and anomalous samples are exploited as training data. The input consists of a multiple two-dimensional time series, each with dimensions $m \times n$, where m represents the time steps and n represents the feature number. The output corresponds to the class label. Anomaly categories are converted into training labels according to Table 1.

To capture distinct anomaly characteristics, we design a new feature combination of seven features, which are LON, LAT, SOG, COG, a, ω, and CLP. Here CLP is the Curvature-Length Product.

4. Numerical results

4.1. Dataset

We evaluate the proposed anomaly detection model on the historical AIS dataset uploaded by the Danish Maritime Authority (DMA, 2023). Considering the geographical conditions off the Denmark coast, vessel activities manifest distinct maneuvering patterns on the western and eastern sides of the continent, resulting in variations in trajectory data of AIS. In the eastern sector, vessels mainly follow established navigational channels, whereas trajectories diverge in the landless western region. Therefore, we choose two separated rectangular AOIs spanning from (56°N, 6.5°E) to (58°N, 8°W) and from (56°N, 11.2°E) to (57.5°N, 12.2°W) for experiments, as illustrated in Fig. 7. The grid size is set at $0.5° \times 0.5°$.

We focus on the AIS data from the tanker and collect the experimental data from 2020 to 2023. The data from January 1, 2020, to December 31, 2022, are employed for model training, and there are 69 538 trajectory entries, with 44 691 of them passing through the eastern region and 49 616 passing through the western region. Model testing is conducted on the data from January 1, 2023, to December 31, 2023. All raw AIS data is filtered and processed following the procedures outlined in Section 3.1.

4.2. Training data preparation

Exploiting the methods proposed in Section 3.3, approximately 5100 SCA points and 2100 TA points are identified. Additionally, 1948 trajectories exhibiting loitering behavior are identified and labeled. To segment the trajectories, we apply the sliding window method with a time step length of 24, corresponding to one hour given a time interval of 150 s between adjacent points, to create the training dataset.

Considering that anomalous points and trajectories constitute a relatively small portion of the entire dataset, a stride size of 1 is chosen for anomalous trajectory sampling. In contrast, regular sampling is used for normal trajectory segment sampling. Trajectories are sliced to create continuous segments, and initially, anomalous points of SCA and TA are detected and labeled. Segments containing no fewer than ϵ anomalous points are identified as anomalies. As the detection threshold ϵ increases, the number of SCA and TA samples decreases and the detection sensitivity of these two types of anomalies rises. Segments comprising only one type of anomalous point are labeled accordingly. In cases where both SCA and TA are present, and the count of TA points equals or exceeds 3, indicating at least one complete and anomalous bend in the trajectory, according to the hierarchy relationship mentioned in Section 3.2, the segment is labeled as TA; otherwise, it is labeled as SCA. Finally, LA samples are obtained manually and annotated.

Considering the imbalanced class distribution across various anomaly types, we employ the compute class weight function from the sklearn library. By adjusting the class weights, reduced model generalization capability arising from the imbalanced class distribution can be effectively addressed.

4.3. Performance evaluation

First, we employ simple structures of Long Short-Term Memory (LSTM) and Gated Recurrent Unit (GRU) networks, along with basic Multi-layer Perceptron (MLP) and Fully Convolutional Networks (FCN). Additionally, for better comparison and performance analysis, LSTM-FCN and GRU-FCN models, which are designed for multivariate time series data classification (Elsayed et al., 2019; Karim et al., 2017), are tested in our experiments. The numerous hyperparameters in neural networks make it complex and inconvenient to manually tune for the globally optimal parameter configuration. Therefore, we perform the Bayesian optimization technique (Nuno et al., 2020) using the Scikit-Optimize library for the optimal combination of hyperparameters.

Second, the F1-score and classification accuracy are utilized to evaluate model performance, calculated as:

$$F1 = \frac{2 \times \text{Precision} \times \text{Recall}}{\text{Precision} + \text{Recall}} \tag{7}$$

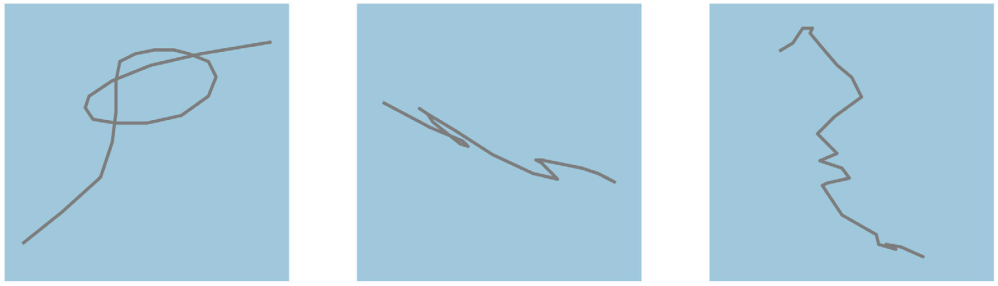

Fig. 6. Three typical shapes of LA examples: (a) Lasso shape; (b) Disordered retracing shape; (c) Zigzagging shape.

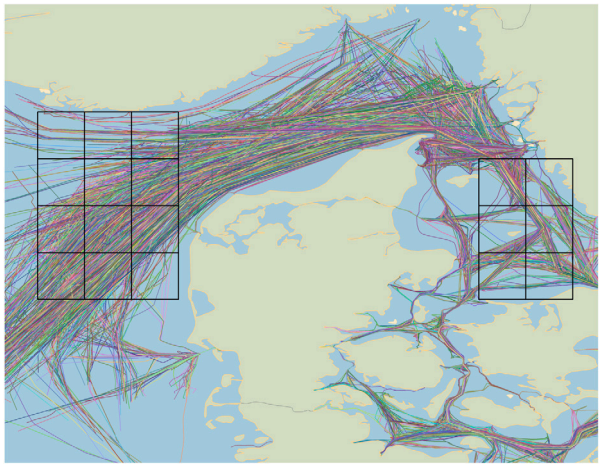

Fig. 7. Processed 5540 trajectories from January 1, 2020, to March 31, 2020, and grid cells established in the western and eastern Areas of Interest (AOI). The western region is configured in areas with dispersed trajectories, while the eastern region is established along several maritime routes. The grid size (latitude × longitude) is $0.5° \times 0.5°$.

Table 2
Changes in the number of SCA and TA samples and detection performance of F1-score with variations in ϵ.

ϵ	SCA		TA	
	Num of samples	F1-score	Num of samples	F1-score
4	3960	99.16%	5891	96.15%
5	1706	93.66%	3747	93.66%
6	796	94.51%	2265	93.58%
7	479	93.60%	1297	89.25%
8	289	95.73%	768	89.35%

$$Accuracy = \frac{TP + TN}{TP + TN + FP + FN} \tag{8}$$

where TP and FP stand for the true positive and the false positive number, respectively. TN and FN stand for the true negative and the false negative number, respectively.

To determine the detection threshold ϵ, we examine the number of samples affected by threshold variations and the corresponding detection performance of LSTM while increasing ϵ, and the results are listed in Table 2. We choose $\epsilon = 6$ because it yields satisfactory detection results for both SCA and TA. However, at the threshold of 4, although it achieves a relatively high F1-score, the high sensitivity in detection may lead to potential drawbacks. Collectively, the overall number of anomalous segments is 5009, and the number of normalcy is about 328,000.

To validate the effectiveness of the proposed method, we conduct two sets of experiments, training our classification models using four features, LAT, LON, SOG, and COG, and using seven features mentioned in Section 3.4, separately. The results are summarized in Table 3.

Table 3
Overall performances of anomaly classification models: (a) Model performances using four-features; (b) Model performances using seven-features.

(a)

Model	F1-score	Accuracy	Training time (min)	Params
LSTM	99.41%	99.36%	3.934	291.8K
GRU	99.41%	99.35%	3.411	**225.8K**
MLP	98.76%	98.46%	**1.467**	301.0K
FCN	99.09%	98.94%	3.451	289.8K
LSTM-FCN	99.17%	99.05%	6.099	558.0K
GRU-FCN	**99.47%**	**99.42%**	5.722	492.0K

(b)

Model	F1-score	Accuracy	Training time (min)	Params
LSTM	**99.79%**	**99.78%**	3.950	294.9K
GRU	99.70%	99.68%	3.473	**228.1K**
MLP	99.26%	99.18%	**1.478**	337.0K
FCN	99.44%	99.40%	3.595	289.8K
LSTM-FCN	99.77%	99.76%	6.532	561.2K
GRU-FCN	99.75%	99.74%	5.992	493.3K

It shows that FCN and MLP achieve relatively poor performance, demonstrating their weakness in handling sequence data modeling tasks compared to RNNs. In contrast, RNNs and hybrid models incorporating RNN demonstrate comparable performance. Notably, in the seven feature experiments, the single-layer LSTM stands out with an F1-score of 99.79%, achieving the best performance, with even the least-performing model yielding an impressive F1-score of 99.70%. While both LSTM-FCN and GRU-FCN achieved acceptable results, they involve more training hyperparameters and demand more training time.

Comparing the results of two feature configurations, models trained with seven features outperform those trained with four features. The fluctuation of F1-score and accuracy in the same model is not entirely proportional to the increase in feature dimensions. This can be attributed to the presence of influential features within the original feature combination, which already strongly contribute to anomaly detection. Thus, while additional features help improve performance, their overall impact on the model may be relatively minor. Despite this, the additional features lead to a decrease in the misclassification rate by approximately 62%.

The confusion matrix in Fig. 8 provides a detailed classification result for the best-performing models in two experimental configurations. In the four-feature setup, there are 379 instances of false alarms, which decreases to 139 when using the seven-feature configuration, indicating a reduction of approximately 63%. Some misclassifications occur probably because these segments exhibit characteristics of two different anomalies simultaneously, leading the model to categorize them as another type of anomaly. The excellent performance in anomaly classification affirms the reliability of the anomaly dataset.

A combination of anomaly detection results is presented in Fig. 9. SCAs frequently occur when vessels conduct unconventional turning

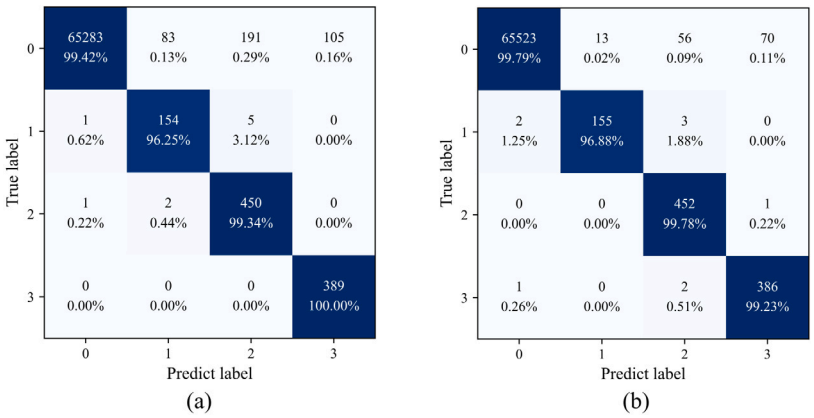

Fig. 8. Confusion matrices for the two best-performing models training with two different feature configurations: (a) GRU-FCN on a 4-feature classification experiment; (b) LSTM on a 7-feature classification experiment. The labels correspond to the mapping relation in Table 1.

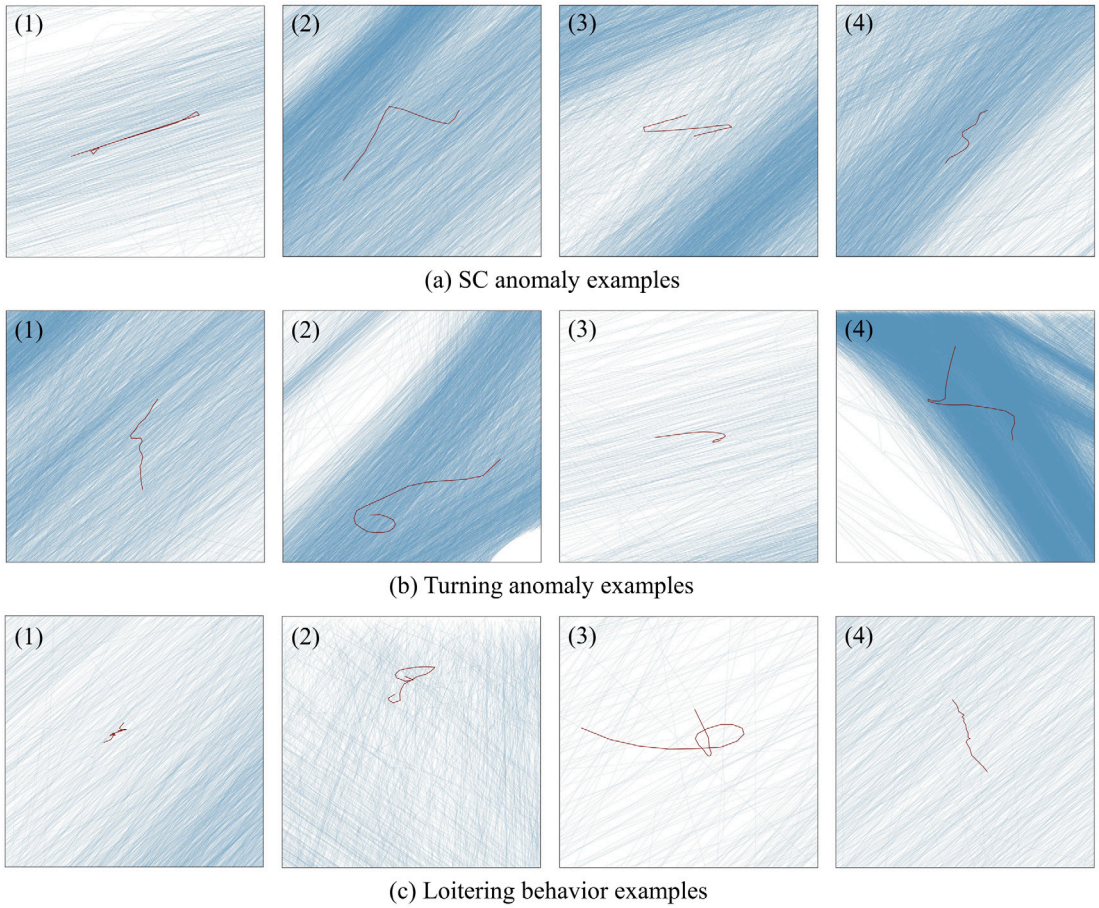

Fig. 9. Examples of anomaly detection results for three types using 2023 AIS data: (a) SCA examples: anomaly caused by abnormal change rate of both speed and course; (b) TA examples: anomaly caused by sharp turns; (c) LA examples: anomaly exhibiting loitering behavior; the size (latitude × longitude) of all subplots in figures a and b is $0.2° \times 0.2°$, and the size of all subplots in figures c is $0.05° \times 0.05°$.

maneuvering, as depicted in Fig. 9a-1, a-2, a-3. Additionally, irregular swinging of vessel trajectories can also lead to anomalies, as illustrated in Fig. 9a-4. All the anomalies presented in Fig. 9(c) are caused by sharp turns at high speeds. Because of the limited traveling distance of loitering vessels, the scale of these trajectories segments in Fig. 9(c) is relatively small. The segment in c-1 represents the disorder retracing shape. c-2 and c-3 are the lasso shape, and c-4 is the zigzagging shape. All loitering segments manifest aimless navigation behavior with high variations in their course and frequent trajectory repetition.

5. Conclusions and discussion

This research introduces a systematic framework for maritime kinematic anomaly detection. Drawing on our understanding of anomalies and considerable sample study, we classify kinematic anomalies into three types and employ distinct detection approaches tailored to their characteristics to establish a reliable labeled anomaly dataset for reference, which significantly reduces the time consumed to label abnormal data, allowing for extensive research into more complicated anomalies. To enhance the accuracy of detection, a novel trajectory feature

combination has been specifically utilized for classification. The experiments are conducted on two separate regions of Denmark, with distinct feature configurations. The new feature configuration outperforms the conventional feature set in LSTM networks classification tasks, achieving an F1-score of 99.79% and reducing the misclassification rate by about 62%. Furthermore, when tested on an additional dataset, our method consistently exhibits promising results, demonstrating its effectiveness in accurately detecting kinematic anomalies. This further validates the robustness of the anomaly dataset generated by our approach.

In this paper, our focus is exclusively on kinematic anomalies. Future work may involve extending the anomaly detection system to encompass other types of anomalies, contributing to the development of a comprehensive maritime anomaly detection framework. Given the variations in anomalies across various ship types, further exploration into diverse vessel behavior, particularly that of fishing vessels, would augment the usability of the system. Another consideration is the utilization of other data types. The research ideas extend beyond AIS data and can also be applied to other sources, such as satellite data, radar data, etc., to create their datasets of anomaly samples. Furthermore, the integration among different datasets provides an integrated scenario to gather supplementary information, contributing to the establishment of a comprehensive framework for anomaly detection. For instance, historical accident data and metocean data can be incorporated to train a classifier for maritime risk analysis through the probability assessment of accidents related to weather conditions (Rawson et al., 2021). Additionally, contextual data, such as archived records, planned paths, and navigational regulations, can be utilized to learn the nominal behavior of vessels for further anomaly detection (Forti et al., 2022). Consequently, our future research will delve deeper into exploring the potential of anomaly detection by leveraging the combined influence of AIS data with other data types. We have chosen two regions off Denmark, representing two vessel motion patterns. Future work will emphasize the application of the proposed system on an extended scale.

CRediT authorship contribution statement

Jinliang Liu: Conceptualization, Formal analysis, Methodology, Software, Visualization, Writing – original draft. **Jianghui Li:** Conceptualization, Formal analysis, Funding acquisition, Methodology, Supervision, Visualization, Writing – review & editing. **Chunshan Liu:** Writing – review & editing, Visualization, Validation, Supervision, Methodology, Funding acquisition, Conceptualization.

Declaration of competing interest

The authors declare that they have no known competing financial interests or personal relationships that could have appeared to influence the work reported in this paper.

Data availability

Data will be made available on request.

References

AGCS, 2023. Safety and shipping review. In: Safety and Shipping Review 2023. pp. 4–5.

Anneken, M., Fischer, Y., Beyerer, J., 2015. Evaluation and comparison of anomaly detection algorithms in annotated datasets from the maritime domain. In: 2015 SAI Intelligent Systems Conference. IntelliSys, IEEE, pp. 169–178.

Arguedas, V.F., Pallotta, G., Vespe, M., 2018. Maritime traffic networks: From historical positioning data to unsupervised maritime traffic monitoring. IEEE Trans. Intell. Transp. Syst. 19, 722–732.

BSI (Ed.), 2013. Maritime Works - General. Code of Practice for Planning and Design for Operations. British Standards Institution.

Bye, R.J., Aalberg, A.L., 2018. Maritime navigation accidents and risk indicators: An exploratory statistical analysis using AIS data and accident reports. Reliab. Eng. Syst. Saf. 176, 174–186.

Capobianco, S., Millefiori, L.M., Forti, N., Braca, P., Willett, P., 2021. Deep learning methods for vessel trajectory prediction based on recurrent neural networks. IEEE Trans. Aerosp. Electron. Syst. 57, 4329–4346.

Chandola, V., Banerjee, A., Kumar, V., 2009. Anomaly detection: A survey. ACM Comput. Surv. 41 (3), 1–58.

Chen, X., Liu, S., Liu, R.W., Wu, H., Han, B., Zhao, J., 2022. Quantifying Arctic oil spilling event risk by integrating an analytic network process and a fuzzy comprehensive evaluation model. Ocean Coast. Manag. 228, 106326.

Chen, X., Liu, S., Zhao, J., Wu, H., Xian, J., Montewka, J., 2024. Autonomous port management based AGV path planning and optimization via an ensemble reinforcement learning framework. Ocean Coast. Manag. 251, 107087.

Chen, X., Wu, H., Han, B., Liu, W., Montewka, J., Liu, R.W., 2023. Orientation-aware ship detection via a rotation feature decoupling supported deep learning approach. Eng. Appl. Artif. Intell. 125, 106686.

Davenport, M., 2008. Kinematic Behaviour Anomaly Detection (KBAD)-Final Report. DRDC CORA report KBAD-RP-52-6615.

DMA, 2023. AIS data. https://dma.dk/safety-at-sea/navigational-information/ais-data.

Elsayed, N., S, A., Bayoumi, M., 2019. Deep gated recurrent and convolutional network hybrid model for univariate time series classification. Int. J. Adv. Comput. Sci. Appl. 10.

Ferreira, M.D., Campbell, J.N.A., Matwin, S., 2022. A novel machine learning approach to analyzing geospatial vessel patterns using AIS data. Gisci. Remote Sens. 59, 1473–1490.

Forti, N., d'Afflisio, E., Braca, P., Millefiori, L.M., Willett, P., Carniel, S., 2022. Maritime anomaly detection in a real-world scenario: Ever given grounding in the Suez Canal. IEEE Trans. Intell. Transp. Syst. 23, 13904–13910.

Guo, S., Mou, J., Chen, L., Chen, P., 2021. An anomaly detection method for AIS trajectory based on kinematic interpolation. J. Mar. Sci. Eng. 9, 609.

Handayani, D.O.D., Sediono, W., Shah, A., 2013. Anomaly detection in vessel tracking using support vector machines (SVMs). In: 2013 International Conference on Advanced Computer Science Applications and Technologies. IEEE, pp. 213–217.

IMO, 1980. International convention for the Safety of Life at Sea (SOLAS). In: Chapter V Safety of Navigation, Regulation 19. pp. 15–16.

Karim, F., Majumdar, S., Darabi, H., Chen, S., 2017. LSTM fully convolutional networks for time series classification. IEEE Access 6, 1662–1669.

Laxhammar, R., 2008. Anomaly detection for sea surveillance. In: 2008 11th International Conference on Information Fusion. IEEE, pp. 1–8.

Laxhammar, R., Falkman, G., Sviestins, E., 2009. Anomaly detection in sea traffic-a comparison of the gaussian mixture model and the kernel density estimator. In: 2009 12th International Conference on Information Fusion. IEEE, pp. 756–763.

Lei, P.-R., Shen, T.-J., Peng, W.-C., Su, J., 2011. Exploring spatial-temporal trajectory model for location prediction. In: 2011 IEEE 12th International Conference on Mobile Data Management. Vol. 1, IEEE, pp. 58–67.

Li, H.H., Liu, J.X., Wu, K.F., Yang, Z.L., Liu, R.W., Xiong, N.X., 2018. Spatio-temporal vessel trajectory clustering based on data mapping and density. IEEE Access 6, 58939–58954.

Liu, B., de Souza, E.N., Hilliard, C., Matwin, S., 2015. Ship movement anomaly detection using specialized distance measures. In: 2015 18th International Conference on Information Fusion. Fusion, IEEE, pp. 1113–1120.

Mascaro, S., Nicholso, A.E., Korb, K.B., 2014. Anomaly detection in vessel tracks using Bayesian networks. Internat. J. Approx. Reason. 55, 84–98.

Miller, N.A., Roan, A., Hochberg, T., Amos, J., Kroodsma, D.A., 2018. Identifying global patterns of transshipment behavior. Front. Mar. Sci. 5.

Nguyen, D., Vadaine, R., Hajduch, G., Garello, R., Fablet, R., 2022. GeoTrackNet–a maritime anomaly detector using probabilistic neural network representation of AIS tracks and a contrario detection. IEEE Trans. Intell. Transp. Syst. 23, 5655–5667.

Nuno, C., Mehdi, C., Alexander, F., Thomas, F., Tim, H., Manoj, K., Gilles, L., Katie, M., Holger, N., Mikhail, P., Iaroslav, S., Taylor, S., Zé, V., 2020. Scikit-optimize.

Pallotta, G., Jousselme, A.-L., 2015. Data-driven detection and context-based classification of maritime anomalies. In: 2015 18th International Conference on Information Fusion. Fusion, IEEE, pp. 1152–1159.

Pallotta, G., Vespe, M., Bryan, K., 2013a. Vessel pattern knowledge discovery from AIS data: A framework for anomaly detection and route prediction. Entropy 15, 2218–2245.

Pallotta, G., Vespe, M., Bryan, K., Ieee, 2013b. Traffic knowledge discovery from AIS data. In: 16th International Conference on Information Fusion. FUSION, pp. 1996–2003.

Park, J., Jeong, J., Park, Y., 2021. Ship trajectory prediction based on bi-LSTM using spectral-clustered AIS data. J. Mar. Sci. Eng. 9.

Rawson, A., Brito, M., Sabeur, Z., Tran-Thanh, L., 2021. A machine learning approach for monitoring ship safety in extreme weather events. Saf. Sci. 141, 105336.

Rhodes, B.J., Bomberger, N.A., Zandipour, M., 2007. Probabilistic associative learning of vessel motion patterns at multiple spatial scales for maritime situation awareness. In: 2007 10th International Conference on Information Fusion. IEEE, pp. 1–8.

Ribeiro, C.V., Paes, A., de Oliveira, D., 2023. AIS-based maritime anomaly traffic detection: A review. Expert Syst. Appl. 120561.

Riveiro, M., Pallotta, G., Vespe, M., 2018. Maritime anomaly detection: A review. Wiley Interdiscip. Rev.-Data Min. Knowl. Discov. 8.

Rong, H., Teixeira, A., Soares, C.G., 2020. Data mining approach to shipping route characterization and anomaly detection based on AIS data. Ocean Eng. 198, 106936.

Roy, J., 2008. Anomaly detection in the maritime domain. In: Optics and Photonics in Global Homeland Security IV. SPIE, pp. 180–193.
Sidibé, A., Shu, G., 2017. Study of automatic anomalous behaviour detection techniques for maritime vessels. J. Navig. 70, 847–858.
Toloue, K.F., Jahan, M.V., 2018. Anomalous behavior detection of marine vessels based on hidden Markov model. In: 2018 6th Iranian Joint Congress on Fuzzy and Intelligent Systems. CFIS, IEEE, pp. 10–12.
UNCTAD, 2022. Review of maritime transport 2022. https://unctad.org/system/files/official-document/rmt2022_en.pdf.
Wang, L.H., Chen, P.F., Chen, L.Y., Mou, J.M., 2021. Ship AIS trajectory clustering: An HDBSCAN-based approach. J. Mar. Sci. Eng. 9.
Wijaya, W.M., Nakamura, Y., 2023. Loitering behavior detection by spatiotemporal characteristics quantification based on the dynamic features of Automatic Identification System (AIS) messages. Peerj Comput. Sci. 9.
Winther, M., Christensen, J.H., Plejdrup, M.S., Ravn, E.S., Eriksson, O.F., Kristensen, H.O., 2014. Emission inventories for ships in the arctic based on satellite sampled AIS data. Atmos. Environ. 91, 1–14.
Xiao, G., Chen, L., Chen, X., Jiang, C., Ni, A., Zhang, C., Zong, F., 2023. A hybrid visualization model for knowledge mapping: Scientometrics, SAOM, and SAO. IEEE Trans. Intell. Transp. Syst. 1–14.
Xu, X., Liu, C., Li, J., Miao, Y., 2022. Trajectory clustering for SVR-based time of arrival estimation. Ocean Eng. 259, 111930.
Xu, X., Liu, C., Li, J., Miao, Y., Zhao, L., 2023. Long-term trajectory prediction for oil tankers via grid-based clustering. J. Mar. Sci. Eng. 11, 1211.
Zhang, Z., Huang, L., Peng, X., Wen, Y., Song, L., 2022. Loitering behavior detection and classification of vessel movements based on trajectory shape and Convolutional Neural Networks. Ocean Eng. 258, 111852.
Zhao, L.B., Shi, G.Y., 2019. Maritime anomaly detection using density-based clustering and recurrent neural network. J. Navig. 72, 894–916.
Zhou, P., Zhao, W., Li, J., Li, A., Du, W., Wen, S., 2020. Massive maritime path planning: A contextual online learning approach. IEEE Trans. Cybern. 51, 6262–6273.